Discretizing the Porous Medium Equation based on its Gradient Flow Structure — A Consistency Paradox.

Thomas Roessler*

12th May 2004

Abstract

A discretization of the Porous Medium Equation that is based on the equation's gradient flow structure is discussed. The resulting numerical scheme uses Lagrangian coordinates. It exhibits good convergence properties near the solution's free boundary which are not predicted by a naive consistency estimate. The seeming paradox is resolved by a heuristic argument.

Mathematics Subject Classification: 35K55, 35R35, 65M99

1 Introduction

We consider the one-dimensional porous medium equation,

$$\rho_t - (\rho^m)_{xx} = 0, \tag{1}$$

for $m > 1$, and discuss a numeric approach based on the gradient flow formulation in [15].

Early approaches for numerically treating the porous medium equation are based on finite-difference schemes. They use Euler coordinates, and have to struggle with the moving free boundary that compactly supported solutions of the porous medium equation exhibit [7]. One remedy for these problems consists in treating the free boundary separately [18, 4], e.g. exploiting analytically known relationships between the pressure's derivative and the speed of the free boundary[1, 9], $\dot{\zeta} = -\frac{m}{m-1}\left(u^{m-1}\right)_x$ [4]. Finite element methods [16, 13, 12] often replace the porous medium equation by a regularized version; these approaches suffer from convergence rates that become arbitrarily low as m is increased. Ebmeyer [5, 6] has

*Institute of Applied Mathematics, University of Bonn, Wegelerstrasse 10, 53115 Bonn, Germany

recently derived a finite element method that does not rely on regularization and yields convergence rates that are bounded from below for large m.

The moving free boundary of solutions to the porous medium equation suggests replacing Euler coordinates by a Lagrange approach. This has first been done by MacCamy, Gurtin and Socolovsky for the case $m = 2$ [11, 8]. They define $X(t, \xi)$ by $X(0, \xi) = \xi; X_t(t, \xi) = -2u_x(X(t, \xi))$. X is then treated by various finite difference and variational approaches. In [3], Budd, Collins, Huang, and Russell rely on a Lagrangian formulation of the porous medium equation. This formulation is combined with various symmetry properties and a first-order discretization of the free boundary's speed. From these ingredients, an equidistant moving mesh is derived that is then used for a fundamentally Eulerian finite difference discretization. In [17], Russo presents a unified discussion of some Lagrangian, Eulerian, and mixed discretizations for the convection-diffusion equation. The purely Lagrangian scheme favored in this paper is applied to the heat equation. The resulting discretization implicitly exploits a gradient flow structure for the heat equation which has been extended to the porous medium equation in [14], and is the basis of the discretization discussed in this paper. In [10], Lions and Mas-Gallic present an analytic convergence proof and numerical experiments for a related method that is obtained by rewriting the porous medium and heat equations as nonlinear transport equations with a smoothened diffusion speed.

2 Gradient Flow Structure

We now proceed by writing the porous medium equation as a gradient flow on the "infinite-dimensional manifold"

$$\mathcal{M} = \left\{ \rho : \mathbb{R} \to \mathbb{R}_0^+, \int \rho = 1 \right\}, \tag{2}$$

with the tangent space

$$T_\rho\mathcal{M} = \left\{ s : \mathbb{R} \to \mathbb{R}, \int s = 0 \right\}. \tag{3}$$

In order to be able to write down the equation of a gradient flow,

$$\operatorname{grad} E(\rho) + \rho_t = 0, \tag{4}$$

we need two key ingredients: A functional E, and a metric tensor g, which associates the (Riemannian) gradient with the functional's differential.

We use Otto's construction [15]: Let $s \in T_\rho\mathcal{M}$. Identify s with some solution p (determined up to an additive constant) of the differential equation

$$s + (\rho p_x)_x = 0. \tag{5}$$

The metric tensor is then defined by

$$g(s_1, s_2) = \int \rho (p_1)_x (p_2)_x \tag{6}$$

We will also use the notation $u = p_x$, and identify s with u. Obviously,

$$s + (\rho u)_x = 0. \tag{7}$$

The energy functional is then defined as

$$E(\rho) = \frac{1}{m-1} \int \rho^m. \tag{8}$$

It can be easily verified that, with these definitions,

$$g(\rho_t, s) + dE.s = 0 \qquad \forall s \in T_\rho \mathcal{M} \tag{9}$$

implies (1). Of course, this equation is just another way to express (4).

3 Discretization

We now exploit the formal gradient flow structure we have just described to construct a discretization of (1).

Fix volumes $V_1 + \cdots + V_N = 1$. For any N consecutive intervals $I_1, \ldots, I_N$ with $I_n = (x_{n-1}, x_n)$, a piecewise constant function h with $h|I_n = V_n/|I_n|$, $h \equiv 0$ elsewhere, can be constructed. Denote the set of all such h as $\mathcal{M}^*$. $\mathcal{M}^*$ can be interpreted as a finite-dimensional Riemannian submanifold of $\mathcal{M}$. Note that each element of $\mathcal{M}^*$ is uniquely determined by the $N+1$ interval boundaries $x_0, \ldots, x_N$. Thus, we can identify $\mathcal{M}^*$ with the convex and open set

$$\{x_0 < x_1 < \cdots < x_N\} \subset \mathbb{R}^{N+1}. \tag{10}$$

Consider $\mathbf{u} = \dot{\mathbf{x}} \in T_{\mathbf{x}}\mathcal{M}$. Under the identification of $T_h\mathcal{M}$ described in the previous section, it can be shown that $\mathbf{u}$ is identified with any continuously differentiable function p for which $p_x(x_n) = u_n$, $p_x|I_n$ linear. We can then use (7) in order to give a matrix representation for the restriction of g to $T\mathcal{M}^*$. Indeed, with $(p_1)_x$, $(p_2)_x$ constructed from $\mathbf{u}^1, \mathbf{u}^2 \in T_{\mathbf{x}}\mathcal{M}^*$,

$$\int \rho (p_1)_x (p_2)_x = \sum_{n=1}^{N} \frac{V_n}{3} \Big(u_n^1 u_n^2 + u_{n-1}^1 u_{n-1}^2 + \frac{1}{2} (u_n^1 u_{n-1}^2 u_n^2 u_{n-1}^1) \Big).$$

Thus, g can be represented as a symmetric tridiagonal matrix M with entries $(V_n/6, V_n/3 + V_{n+1}/3, V_{n+1}/6)$.

Expressing the energy functional and its derivatives in coordinates is straight forward:

$$E(x) = \frac{1}{m-1} \sum \frac{V_n^m}{|I_n|^{m-1}}, \tag{11}$$

$$\frac{\partial E}{\partial x_n} = -\frac{V_n^m}{|I_n|^m} + \frac{V_{n+1}^m}{|I_{n+1}|^m}. \tag{12}$$

We now have all ingredients to write the restriction of (4) to $\mathcal{M}^*$ as a system of ordinary differential equations: Denoting the Euclidean gradient operator on $\mathbb{R}^{N+1}$ as ∇, we can write

$$\nabla E(\mathbf{x}) + M\dot{\mathbf{x}} = 0. \tag{13}$$

Finally, we have to construct a projection $\Pi : \mathcal{M} \to \mathcal{M}^*$: Consider a function $\rho \in \mathcal{M}$. Then we select $\mathbf{x} = \Pi(\rho)$ so that

$$\int_{x_{n-1}}^{x_n} \rho(x)dx = V_n. \tag{14}$$

Consider any curve $t \mapsto \rho(t) \in \mathcal{M}$, and, with the usual identification of the tangent space, associate $u = p_x$ with $\dot{\rho}$. Define the curve $\mathcal{M}^* \ni \mathbf{x}(t) := \Pi(\rho(t))$. It is then easy to show that, for every t, $u_n := \dot{x}_n = u(x_n)$.

4 Consistency

In order to understand the relationship between solutions to (1) and (13), we consider some solution $\rho(t,x)$ of (1), and use the discretization as initial data for the system of ordinary differential equations (13), $\mathbf{x} = \Pi(\rho)$. From (13), we obtain the "discrete" value of $\dot{\mathbf{x}}$, call it $\mathbf{v}$,

$$\nabla E\left(\Pi(\rho)\right) + M\mathbf{v} = 0, \tag{15}$$

which has, for fixed t, to be compared to the "continuous" value $\mathbf{u}$ of $\dot{\mathbf{x}}$, $\mathbf{u} = \frac{d}{dt}\left(\Pi(\rho(t))\right)$. Indeed, we have

$$M(\mathbf{u} - \mathbf{v}) = \nabla E(\mathbf{x}) + M\mathbf{u} =: \mathbf{r}. \tag{16}$$

Note that $\mathbf{r}$ actually represents an object in $\mathcal{M}^*$'s cotangent space. We will later have to transform it back into $T\mathcal{M}^*$.

$\mathbf{u}$ can immediately be expressed in terms of ρ: We have $u_n = u(x_n)$,

$$\rho_t - m(\rho^{m-1}\rho_x)_x = 0, \tag{17}$$

$$\rho_t + (\rho u)_x = 0. \tag{18}$$

Then,

$$u_n = -m\rho^{m-2}(x_n)\rho_x(x_n). \tag{19}$$

For $\nabla E(\mathbf{x})$, we use (12).

We now introduce "volumetric" coordinates: For $W \in [0,1]$, define $x(W)$ by

$$\int_0^{x(W)} \rho(\xi)d\xi = W. \tag{20}$$

Using $\rho = (dx/dW)^{-1}$, we can now rewrite u:

$$u = -m\rho^{m-2}\rho_x = -\frac{d}{dW}\left(\frac{dx}{dW}\right)^{-m} \tag{21}$$

Introducing the notation $W_n := \sum_{k=1}^{n} V_k$, we also notice that $|I_n|/V_n$ is a difference quotient approximating $x'(W_n)$. We proceed by demonstrating that

$$\begin{aligned}(M\mathbf{u})_n &\approx -\frac{V_n + V_{n+1}}{2}\frac{d}{dW}\left(\frac{dx}{dW}\right)^{-m}\\ &\approx -\left(\frac{|I_{n+1}|}{V_{n+1}}\right)^{-m} + \left(\frac{|I_n|}{V_n}\right)^{-m}\\ &= -\frac{\partial E}{\partial x_n}\end{aligned}$$

1. We have the identity

$$(M\mathbf{u})_n = -\frac{V_n}{6}((x')^{-m})'(W_{n-1}) - \frac{V_n + V_{n+1}}{3}((x')^{-m})'(W_n) - \frac{V_n}{6}((x')^{-m})'(W_{n+1}).$$

Note that

$$((x')^{-m})'(W_n) - ((x')^{-m})'(W_{n-1}) = ((x')^{-m})''(W_n)V_n + \mathcal{O}(((x')^{-m})'''V_n^2),$$

where $((x')^{-m})'''$ is evaluated somewhere in (W_{n-1}, W_n). This yields the following error estimate:

$$\begin{aligned}(M\mathbf{u})_n = &-\frac{V_n + V_{n+1}}{2}((x')^{-m})'(W_n) + \frac{V_n^2 - V_{n+1}^2}{6}((x')^{-m})''(W_n)\\ &+\mathcal{O}(((x')^{-m})'''(V_n^3 + V_{n+1}^3))\end{aligned}$$

2. Expand x into a Taylor series around W_n. Then,

$$\begin{aligned}\frac{|I_n|}{V_n} &= x'(W_n) - \frac{1}{2}x''(W_n)V_n + \frac{1}{6}x'''(W_n)V_n^2 + \mathcal{O}(x^{(4)}V_n^3),\\ \frac{|I_{n+1}|}{V_{n+1}} &= x'(W_n) + \frac{1}{2}x''(W_n)V_{n+1} + \frac{1}{6}x'''(W_n)V_{n+1}^2 + \mathcal{O}(x^{(4)}V_{n+1}^3).\end{aligned}$$

Using these expressions, we now expand $(|I_n|/V_n)^{-m}$ and $(|I_{n+1}|/V_{n+1})^{-m}$ into Taylor series around $x'(W_n)$. We obtain the following expression:

$$\begin{aligned}
&\left(\frac{|I_{n+1}|}{V_{n+1}}\right)^{-m} - \left(\frac{|I_n|}{V_n}\right)^{-m} \\
&= -m(x'(W_n))^{-m-1}\Big(x''(W_n)\frac{V_n + V_{n+1}}{2} + \frac{1}{6}x'''(W_n)(V_{n+1}^2 - V_n^2) + \mathcal{O}(x^{(4)}(V_{n+1}^3 + V_n^3))\Big) \\
&\quad + \frac{m(m+1)}{2}(x'(W_n))^{-m-2}\Big(\frac{1}{4}(x''(W_n))^2(V_{n+1}^2 - V_n^2) + \mathcal{O}(x''x'''(V_n^3 + V_{n+1}^3))\Big) \\
&\quad + \mathcal{O}((x')^{-m-3}(x'')^3(V_n^3 + V_{n+1}^3)) \\
&= ((x')^{-m})'(W_n)\frac{V_n + V_{n+1}}{2} + \cdots
\end{aligned}$$

Provided that $x(W)$ is sufficiently regular and that the V_n are selected in such a way that

$$(V_n^2 - V_{n+1}^2) = \mathcal{O}(V_n^3 + V_{n+1}^3),$$

we have shown that the "dual" consistency error r_n is of order V_n^3.

Transforming back from the cotangent into the tangent space, we obtain a consistency error of $\mathcal{O}(V_n^2)$. (Just note that the diagonal elements of M^{-1} are of order V_n^{-1}, and that matrix elements of that inverse decay exponentially in their distance from the diagonal.)

In practice, however, solutions of the porous medium equation will exhibit singular behaviour near the free boundary: Consider, for instance, the traveling wave ansatz $\rho(x,t) \sim (x-ct)^\alpha$. Inserting this into (1), we obtain the necessary contdition $\alpha = \frac{1}{m-1}$. Note that this is also the kind of boundary behavior the explicitly known self-similar Barenblatt solution [2] of (1) exhibits.

Assume that, near the boundary, $\rho(x) \sim x^{\frac{1}{m-1}}$. In volumetric coordinates, this means $x \sim W^{\frac{m-1}{m}}$ and $\rho \sim W^{1/m}$. Calculating derivatives and inserting the results into our estimates, we obtain the following expression for r_n:

$$r_n \sim W_n^{-1}(V_{n+1}^2 - V_n^2) + W_n^{-2}(V_n^3 + V_{n+1}^3) \tag{22}$$

Note, in particular, what happens for $n \to 0$: In this case, we have $W_n \sim V_n$, which imples $r_n \sim V_n$ for small n. (For $n = 1$, this estimate has to be proven separately for $\partial E/\partial x_n$ and $(M\mathbf{u})_n$. We omit the details for brevity.)

In terms of the tangent space, this means that we seem to have no consistency at all at the free boundary, while we have consistency of order two in the interior of ρ's support.

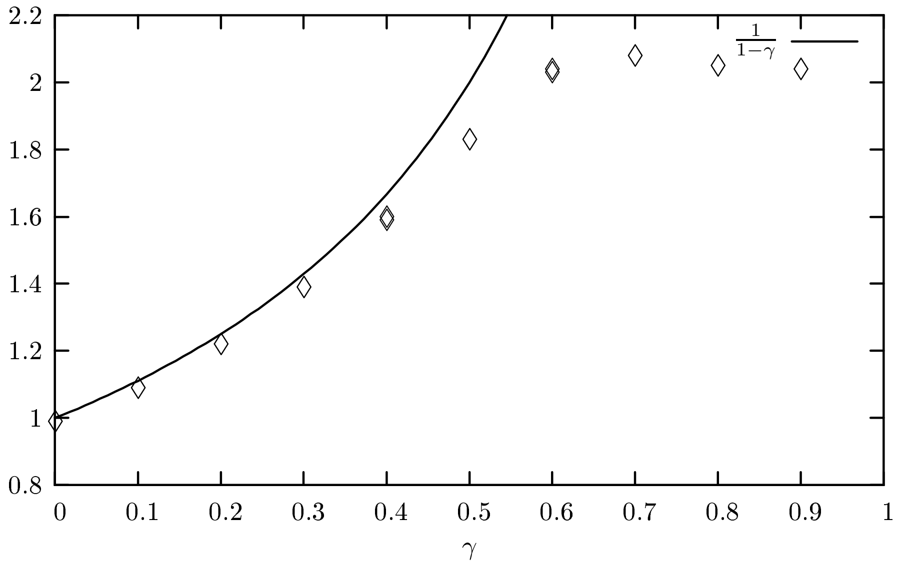

Figure 1: Convergence order of the free boundary.

5 Numerics

In order to numerically investigate this boundary behavior, we discretize the Barenblatt solution for $m = 4$ as described above. We then use a semi-implicit time step to solve the discretized problem for a number of time steps, and investigate the convergence of the free boundary.

Even before we consider the quantitative numerical results, we note that, qualitatively, the solution of the discretized problem (including the free boundary) seems to evolve in a self-similar manner, and according to the same scaling law as the Barenblatt solution — at least after a short initial phase in which the free boundary seems to move "too slowly."

The experimentally determined order of convergence of the free boundary can be found in figure 5.

For an equidistant partition ($|I_n| = d =$ const.), the free boundary shows convergence of order $\mathcal{O}(d)$.

We then introduce partitions which are getting finer as the free boundary is approached: Fix $\gamma \in [0, 1)$, and choose coordinates so the lower free boundary is at $x = 0$. Select x_n with $x_n - x_{n-1} = x_n^\gamma d$. Proceed analogously for the upper free boundary. By integrating Z with $Z|I_n = 1/|I_n|$ over $(0, 1)$, it can be seen that the number of intervals obtained this way behaves like $\frac{1}{d(1-\gamma)}$.

Numerical experiments show that the order of convergence of the free boundary is approximately $\frac{1}{1-\gamma}$ for $\gamma < \frac{1}{2}$, and approaches a constant value of 2 for $\gamma \geq \frac{1}{2}$.

The upper bound of 2 for the order of convergence is plausible from our consistency estimates.

However, from our earlier consistency estimate it seems paradox that the free boundary converges at all.

6 Resolving the paradox

We give a heuristic argument which may help to resolve this observation.

Otto shows in [15] that a self-similar solution of (1) can be characterized by saying that its profile is the minimizer of the modified energy functional

$$F(\rho) = \frac{1}{m-1}\int \rho^m dy + \frac{\alpha}{2}\int \rho y^2 dy, \tag{23}$$

with $\alpha = \frac{1}{m+1}$. For any given $\rho(t,x)$, the profile $\hat{\rho}(\tau, y)$ is defined by setting $t = \exp\tau$, $x = t^\alpha y$, $\hat{\rho}(\tau, y) = t^\alpha \rho(t,x)$.

This characterization can be readily applied to the discrete case: There exists, on any given $\mathcal{M}^*$, a unique minimizer to (23). For this minimizer, $\mathbf{r} = 0$ (see (16)).

One possible interpretation of the convergence rates observed in numerical experiments is the following: The self-similar solution of the discrete problem is close, but not identical to the discretization of the Barenblatt solution. It is the convergence between these two profiles that we are observing. In what follows, we give an approximative argument for the order with which the free boundary of the self-similar solution of the discretized problem converges to the Barenblatt solution's free boundary.

Let $\mathbf{y}$ be the "profile" of the discretized Barenblatt solution, and let $\mathbf{y}^*$ be the minimizer of the restriction of F to $\mathcal{M}^*$. We want to use the consistency estimates (22) to obtain information about $\mathbf{y} - \mathbf{y}^*$, or, more precisely, the first component of this expression which actually describes the free boundary's behavior.

We have the following equations:

$$\begin{aligned} \operatorname{diff} E(\mathbf{y}^*) + \alpha M \mathbf{y}^* &= 0, \\ \operatorname{diff} E(\mathbf{y}) + \alpha M \mathbf{y} &= \mathbf{r} \end{aligned}$$

Subtraction leads to:

$$\operatorname{diff} E(\mathbf{y}) - \operatorname{diff} E(\mathbf{y}^*) + \alpha M(\mathbf{y} - \mathbf{y}^*) = \mathbf{r} \tag{24}$$

To deal with this equation, we perform three approximations: First, we linearize by performing a first-order expansion around $\mathbf{y}^*$. Second, we "continualize" and replace the linearized discrete equation by a linear ordinary differential equation. Third, we focus our attention on the behaviour of that equation's solution near the left boundary of its support.

1. Expanding (24) around $\mathbf{y}^*$ to first order yields:

$$(\operatorname{Hess} E(\mathbf{y}^*) + \alpha M)(\mathbf{y} - \mathbf{y}^*) \approx \mathbf{r} \tag{25}$$

2. Instead of inverting the matrix in this equation, we deduce an ordinary differential equation in volumetric coordinates. First, we test (25) with an arbitrary $\tilde{u} \in T_{\mathbf{y}^*}\mathcal{M}^*$ and obtain the following formal equation:

$$\langle \mathbf{r}, \tilde{u} \rangle = \operatorname{Hess} E\Big|_{\mathbf{y}^*}(\mathbf{y} - \mathbf{y}^*, \tilde{\mathbf{u}}) + \alpha g(\mathbf{y} - \mathbf{y}^*, \tilde{\mathbf{u}}) \tag{26}$$

Consider the individual expressions in this equation: The metric is replaced by an L^2 scalar product upon transition to volumetric coordinates, since $dV = \rho\, dx$. The Hessian has to be replaced by the expression

$$\operatorname{Hess} E(\tilde{u}, \tilde{u}) = \\ -m \int \frac{d}{dV}\left[\left(\frac{dx}{dV}\right)^{-(m+1)} \frac{d\tilde{u}}{dV}\right] \tilde{u}\, dV.$$

Finally, $\langle \mathbf{r}, \tilde{u} \rangle$ must be replaced by a scalar product $\int r(V)\tilde{u}(V)dV$, where the function r must be selected appropriately.

Except for constant multipliers, we obtain the following ordinary differential equation:

$$-\frac{d}{dV}\left(\left(\frac{dx}{dV}\right)^{-m-1} \frac{dR}{dV}\right) + R(V) = r(V) \tag{27}$$

3. We're interested in the behavior of R for $V \to 0$, i.e., near the left free boundary. The self-similar profile can be approximated by $x(V) \sim V^{\frac{m-1}{m}}$. $r(V)$ must be chosen to describe the asymptotic behaviour of (22) near the free boundary. Under the assumption that $V_n^2 - V_{n-1}^2 \sim W_n^{-1} V_n^3$, (22) turns into $r_n \sim W_n^{-2} V_n^3$. With the refinement $x_n - x_{n-1} = x_n^\gamma d$, we obtain $V_n \sim x(W_n)^{\frac{1}{m-1}} x(W_n)^\gamma d$. The appropriate expression for r is then:

$$r(W) = \underbrace{W^{-2}}_{\sim W_n^{-2}} \underbrace{\left(x(W)^{\frac{1}{m-1}} x(W)^\gamma d\right)^2}_{\sim V_n^2} \tag{28}$$

(Note that the exponent on the V_n term is lowered by one to account for the metric tensor's contribution to r_n.)

Plugging these expressions into (27), we have

$$-\frac{d}{dV}\left(V^{\frac{m+1}{m}} \frac{dR}{dV}\right) + R(V) \sim V^{(-2+2\gamma)\frac{m-1}{m}} d^2. \tag{29}$$

Instead of formally solving this equation, we make the power law ansatz $R(W) \sim W^\alpha d^2$ for $W \to 0$. Free boundary convergence of second order then corresponds to an exponent $\alpha \geq 0$. We have the following condition:

$$V^{\alpha-2+\frac{m+1}{m}} + V^\alpha \sim V^{(-2+2\gamma)\frac{m-1}{m}} \tag{30}$$

Comparing the exponents of dominating terms, we get $\alpha = (2\gamma - 1)\frac{m-1}{m}$. $\alpha \geq 0$ thus corresponds to $\gamma \geq \frac{1}{2}$.

This — heuristic! — finding is consistent with the results of our numerical experiments.

References

[1] D. G. Aronson. Regularity properties of flows through porous media: The interface. *Arch. Rational Mech. Anal.*, 37:1–10, 1970.

[2] G. I. Barenblatt. On self-similar motions of a compressible fluid in a porous medium. *Akad. Nauk SSSR. Prikl. Mat. Meh.*, 16:679–698, 1952.

[3] C. J. Budd, G. J. Collins, W. Z. Huang, and R. D. Russell. Self-similar numerical solutions of the porous-medium equation using moving mesh methods. *R. Soc. Lond. Philos. Trans. Ser. A Math. Phys. Eng. Sci.*, 357(1754):1047–1077, 1999.

[4] E. DiBenedetto and David Hoff. An interface tracking algorithm for the porous medium equation. *Trans. Amer. Math. Soc.*, 284(2):463–500, 1984.

[5] Carsten Ebmeyer. *Konvergenzraten Finiter Elemente für die Poröse-Medien-Gleichung im* $\mathbf{R}^n$. PhD thesis, Rheinische Friedrich-Wilhelms-Universität zu Bonn, 1996.

[6] Carsten Ebmeyer. Error estimates for a class of degenerate parabolic equations. *SIAM J. Numer. Anal.*, 35(3):1095–1112 (electronic), 1998.

[7] J. L. Graveleau and P. Jamet. A finite difference approach to some degenerate non-linear parabolic equations. *SIAM J. Appl. Math.*, 20:199–223, 1971.

[8] Morton E. Gurtin, Richard C. MacCamy, and Eduardo A. Socolovsky. A coordinate transformation for the porous media equation that renders the free boundary stationary. *Quart. Appl. Math.*, 42(3):345–357, 1984.

[9] Barry F. Knerr. The porous medium equation in one dimension. *Trans. Amer. Math. Soc.*, 234(2):381–415, 1977.

[10] Pierre-Louis Lions and Sylvie Mas-Gallic. Une méthode particulaire déterministe pour des équations diffusives non linéaires. *C. R. Acad. Sci. Paris Sér. I Math.*, 332(4):369–376, 2001.

[11] R. C. MacCamy and Eduardo Socolovsky. A numerical procedure for the porous media equation. *Comput. Math. Appl.*, 11(1-3):315–319, 1985. Hyperbolic partial differential equations, II.

[12] R. H. Nochetto. On fixed domain approximations to free boundary problems with interface estimates. In *Free boundary problems: theory and applications, Vol. II (Irsee, 1987)*, pages 628–635. Longman Sci. Tech., Harlow, 1990.

[13] Ricardo H. Nochetto and Claudio Verdi. Approximation of degenerate parabolic problems using numerical integration. *SIAM J. Numer. Anal.*, 25(4):784–814, 1988.

[14] Felix Otto. The geometry of dissipative evolution equations: the porous medium equation. *Comm. Partial Differential Equations*, 26(1-2):101–174, 2001.

[15] Felix Otto. The Geometry of Dissipative Evolution Equations: The Porous Medium Equation. *Comm. Part. Diff. Eq.*, 26:101–174, 2001.

[16] Michael E. Rose. Numerical methods for flows through porous media. I. *Math. Comp.*, 40(162):435–467, 1983.

[17] Giovanni Russo. Deterministic diffusion of particles. *Comm. Pure Appl. Math.*, 43(6):697–733, 1990.

[18] Kenji Tomoeda and Masayasu Mimura. Numerical approximations to interface curves for a porous media equation. *Hiroshima Math. J.*, 13(2):273–294, 1983.